Formulas for the force dipole interaction of surface line defects in homoepitaxy

2010 J. Phys. A: Math. Theor. 43 455001

(http://iopscience.iop.org/1751-8121/43/45/455001)

J. Phys. A: Math. Theor. **43** (2010) 455001 (20pp) doi:10.1088/1751-8113/43/45/455001

Formulas for the force dipole interaction of surface line defects in homoepitaxy

John Quah[1], **Li Peng Liang**[2] **and Dionisios Margetis**[3,4,5]

[1] 7201 Claymore Ave, Hyattsville, MD 20782, USA
[2] Department of Physics, Engineering and Geosciences, Montgomery College, Rockville, MD 20850, USA
[3] Department of Mathematics, University of Maryland, College Park, MD 20742, USA
[4] Institute for Physical Science and Technology, University of Maryland, College Park, MD 20742, USA
[5] Center for Scientific Computation and Mathematical Modeling, University of Maryland, College Park, MD 20742, USA

E-mail: dio@math.umd.edu

Received 19 April 2010, in final form 31 August 2010
Published 19 October 2010
Online at stacks.iop.org/JPhysA/43/455001

Abstract

Using asymptotics, we derive explicit, simplified formulas for integrals representing the *force dipole interaction energy per unit length* between line defects (steps) of the same sign that form perturbations of circles in homoepitaxy. Our starting point is continuum linear elasticity in accordance with the classic model by Marchenko and Parshin (1981 *Sov. Phys.—JETP* **52** 129). In the case with concentric circular steps, we define a small geometric parameter, δ^2, which expresses the smallness of interstep distance relative to the circle radii. We invoke the Mellin transform with respect to δ^2 and derive systematically an approximation for the requisite integral. This technique offers an alternative to an exact evaluation in terms of elliptic integrals. We then demonstrate the use of the Mellin transform when calculating the force dipole interaction energy between smoothly, slowly varying steps that form perturbations of circles. We discuss the implications of our results for small-amplitude modulations of circular step profiles.

PACS numbers: 68.35.Md, 81.10.Aj, 62.20.D-, 02.30.Mv, 02.30.Uu, 68.35.-p

1. Introduction

Modern small devices rely on the precise patterning of crystal surfaces to create nanostructures and thin films with desired properties. Below the roughening transition temperature, typical crystal surfaces are not atomically flat, but instead consist of nanoscale terraces separated by line defects, i.e. steps of atomic height [1]. The interaction between steps plays a prominent role in surface morphological evolution.

Fundamental studies of step interactions include the model by Marchenko and Parshin (MP) [2], where each step is viewed as a distribution of force *dipoles* in the context of continuum elasticity (see also [3]). This model describes elastic step energies in *homoepitaxy*, where the last layer of the crystal has the same equilibrium structure as the bulk. The interaction energy of two (infinitesimal) force dipoles at distance R decays as R^{-3}. This behavior is contrasted with the elastic interaction energy arising in *heteroepitaxy*, where steps amount to force monopoles [4, 5]. Effects such as atomic-scale roughness [6], elastic anisotropy [7] and surface elasticity under concentrated normal and shear loads [8] have enriched the MP model. Germane computations address mainly interactions between *straight* steps. In more complicated geometries, the requisite integrals may have an intricate dependence on the physical parameters.

In this paper, we focus on force dipole interactions between two-dimensional (2D) steps of the same sign in homoepitaxy. We consider configurations that allow for simplified (yet nontrivial) approximations. By using smooth and slowly varying step profiles that form *perturbations of concentric circles*, we illustrate analytically the calculation of force dipole step interaction energies. Our resulting, explicit formulas aim to complement thermodynamic ingredients of step flow models describing crystal surface morphological evolution near equilibrium [1]. Such models are invoked extensively in the simulation and analysis of the motion of *many steps*. As an implication, we discuss elastic energy variations via small-amplitude modulations of concentric circular steps.

The basic ingredients of step flow were introduced by Burton, Cabrera and Frank (BCF) [9]. In their pioneering work, the steps are non-interacting. Since then, progress has been made in illustrating how to compute the interaction energies between steps of reasonably arbitrary shapes; for related reviews see, e.g., [1, 4, 10–12].

In particular, modulations of *straight* steps are studied by Houchmandzadeh and Misbah [4] via isotropic elasticity in homoepitaxy and heteroepitaxy. In the former case, the authors conclude that the elastic interaction may favor a modulated step profile for sufficiently large wavelengths.

Our intention is to demonstrate a method for computing force dipole interactions of a class of step profiles in two space dimensions. This tool is the Mellin transform with respect to a suitable geometric parameter. Our setting involves perturbations of circular steps, thus differing from that in [4]. Applications of the Mellin transform, although known in the context of acoustics and electromagnetism [13] and high-energy particle scattering [14], seem to have been previously unexplored in materials physics. Our analysis reveals some radial *asymmetry* effects of the perturbed steps.

The step flow equations are usually rotationally symmetrical and, thus, allow for global rotational symmetry if the initial step configuration consists of concentric circles. Our setting is relevant to possible *deviations* from this symmetry, which can be caused by additional effects in the governing equations or the initial data. Furthermore, the ensuing computation of elastic dipole interaction energies for modulated step profiles can help explore possibilities for energetically favorable configurations in homoepitaxy.

A detailed exposition on force dipole interactions between steps in the context of one-dimensional (1D) geometries is given by Pimpinelli and Villain [15]. They motivate and define the respective energy per unit length for straight steps via the MP model [2]. This energy decays as w^{-2} where w is the terrace width. The connection of force dipole step energies to the requisite principles of continuum elasticity is elucidated in [15].

In this paper, we start with concentric circular steps whose radii are sufficiently large. A previously used formula for the leading-order asymptotic term of the force dipole interaction energy of steps in this geometry exhibits a simple geometric factor [16]. This formula

has been adopted by some works on crystal surface morphological evolution [17–21]. We derive this formula explicitly by invoking the MP model of interacting force dipoles and asymptotics following our definition of a small geometric parameter. This parameter expresses the smallness of the interstep distance relative to the step radii. The example of concentric circles serves as a guide for more complicated cases, e.g. perturbed circular steps, which we examine here.

To approximate the requisite integrals in the non-radial case, we apply the Mellin transform with respect to an analogous geometric parameter. This technique offers a streamlined procedure for obtaining distinct terms in an asymptotic series for the force dipole interaction energy. Using the Mellin transform, asymptotic terms of different orders come from residues of distinct poles of the transformed function. An alternate method invokes elliptic integrals (see section 3 and appendix A in connection to the radial case).

Our broader goal is to tackle the question: *how do the shapes of steps affect their elastic interaction energy?* We focus primarily on the force dipole energy *per unit step length*. This quantity enters the step chemical potential of BCF-type models [1]. The dependence on geometry of an approximation for this interaction energy has been attributed to a geometric factor Φ [22], by analogy with concentric circular steps [16]. In [22], from the use of local coordinates perpendicular and parallel to step edges, this Φ is assumed to depend locally on the transverse coordinates of the interacting steps. For the perturbed geometries considered here, this hypothesis for the leading-order term is reasonable. The next higher order term is logarithmic in the interstep distance, with a prefactor depending on local geometric features (e.g. curvature) of the adjacent step curve.

We discuss the total force dipole interaction energy of modulated concentric steps with reference to their unperturbed circular geometry. Our computation indicates that for a fixed wavenumber, this elastic contribution to the energy does not favor modulations, regardless of the relative phase shift between the interacting steps. This situation may change for large wavenumbers, which lie outside the scope of our asymptotics.

Our results rest on several simplifying assumptions. First, the strain field due to a step edge is obtained as a *superposition* of the dipole strain fields arising from each point of the step edge. So, the material behavior is supposed to be in the *linear elastic* regime. Second, the force dipole moment associated with each point of a step edge has a negligible (z-)component normal to the reference plane. In the same vein, we regard as constant the force dipole moment per unit step length. The geometries chosen are consistent with slowly varying step configurations [22], where the associated curvatures change appreciably over lengths comparable to a macroscopic length. We neglect entropic step repulsions, since at sufficiently low manufacturing temperatures of interest, the thermal wandering of steps [1] tends to be suppressed. We repeat that heteroepitaxy, where steps form force monopole distributions, is not addressed here.

The remainder of the paper is organized as follows. In section 2, we review some background for the motion of crystal steps, and discuss the role of step interactions. In section 3, we demonstrate the application of the associated formula to the calculation of force dipole step interactions in one coordinate, including concentric circular steps (radial case) and a simple variant of their geometry. In section 4, we allow the curvature of steps to vary slowly. Finally, in section 5 we discuss our results.

2. Background

In this section we introduce the geometry and review the basics of force dipole step interactions. The geometry of crystal steps is depicted from two perspectives in figure 1. The cross-sectional

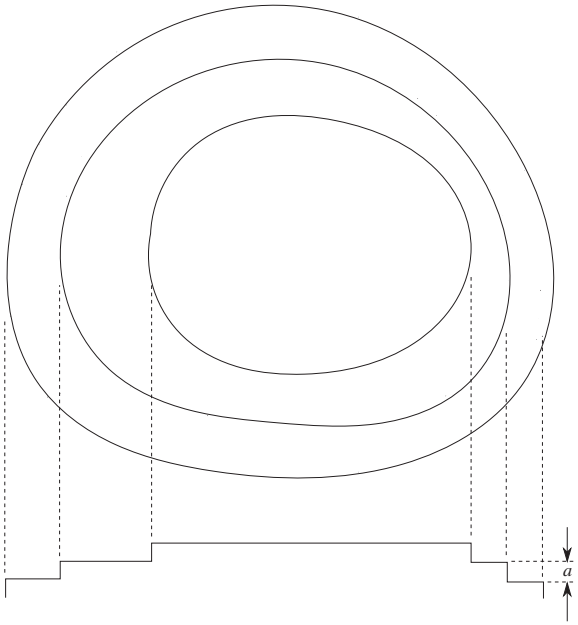

Figure 1. 2D steps. Top: projection on the reference plane. Bottom: cross section.

view illustrates steps of atomic height, a, that descend from a surface peak. The steps are projected onto non-crossing, non-self-intersecting, smooth curves on the reference ('basal') plane[6], shown in the upper part of figure 1. In the radial case studied, e.g. in [17, 19], these curves are concentric circles.

To place step interactions in the broader context of crystal surface motion, we briefly discuss elements of BCF-type models[7]. Then, we review the main ideas underlying the modeling of interacting steps by force dipoles.

2.1. Evolution of crystal surfaces: role of step interactions

In surface diffusion, the motion of steps is mediated by diffusion of adsorbed atoms (adatoms) on terraces between steps, and by attachment and detachment of adatoms at step edges. Each step moves by mass conservation, since the step velocity balances out mass fluxes. Specifically, in the absence of edge atom diffusion [1, 23], the normal velocity of each step is simply the difference of terrace adatom normal fluxes.

The atom attachment–detachment at step edges is expressed through appropriate boundary conditions for the adatom diffusion equation. By linear kinetics [1], the adatom flux normal to the jth step edge is proportional to the difference of the terrace adatom density from an *equilibrium* adatom density, C_j^{eq}. This C_j^{eq} quantifies the propensity of a step edge to incorporate or release atoms. By recourse to notions of thermodynamic equilibrium, this

[6] The usual requirement of continuously differentiable curves would suffice for normal and tangent vectors to be well defined at each point of the step curve. Here, we impose the stronger condition of *infinitely* differentiable (smooth) curves since this is in principle necessary for asymptotics (by our method) to *arbitrary* order in the small geometric parameter (to be defined below).

[7] As mentioned in section 1, in the BCF theory [9] steps are non-interacting.

propensity is expressed by the law [1] $C_j^{\rm eq} = C^0 \exp\left[\mu_j/(k_B T)\right]$ where μ_j is the step chemical potential (a thermodynamic force), $k_B T$ is the Boltzmann energy and C^0 is a constant.

This μ_j is the *change of the jth-step energy per atom captured or released by the step edge* and links step motion to energetics [22]. It can be shown that μ_j involves the step curvature (line tension), entropic step repulsion and elastic step interaction [1, 24]. The entropic and force dipole interaction energies per unit step length decay as the inverse square of step separation in the case of infinitely straight steps [15, 24].

In the radial case, the step chemical potential is [16, 19, 20][8]

$$\mu_j = \frac{\Omega g_1}{r_j} + \frac{\Omega}{a r_j}\frac{\partial}{\partial r_j}\{r_j[V(r_j, r_{j+1}) + V(r_{j-1}, r_j)]\}, \tag{1}$$

where Ω is the atomic volume, g_1 expresses the line tension, r_j are the radii of concentric circles and $V(r_j, r_{j+1})$ is the pairwise interaction energy between steps j, $j+1$ *per unit length of step j*. By [16, 19], for force dipole repulsion in homoepitaxy, this V is

$$V(r_j, r_{j+1}) = g\,\frac{2r_{j+1}}{r_j + r_{j+1}}\left(\frac{a}{r_{j+1} - r_j}\right)^2, \tag{2}$$

where $g > 0$ and measures the strength of each elastic dipole. Formula (2) is derived by the Mellin transform in section 3.2 (see appendix A for an alternate derivation).

It is worthwhile adding an extension of (1) to non-radial geometries. If U_j is the energy per unit length of step j, it has been shown [22] that

$$\mu_j = (\Omega/a)\left(\xi_\eta^{-1}\partial_{\eta_j} U_j + \kappa_j U_j\right), \tag{3}$$

where $\eta = \eta_j$ is a local curvilinear coordinate specifying step j, $\xi_\eta = |\partial_\eta \mathbf{r}|$ is a metric coefficient ($\mathbf{r}$: position vector of the basal plane) and κ_j is the step curvature. Thus, it is expedient to compute the quantity U_j in terms of step coordinates.

We conclude this subsection by revisiting the derivation of (3) [22]. Consider the coordinates (η, σ) where σ indicates position along a fixed step edge ($\eta = \eta_j$) with the metric coefficient $\xi_\sigma = |\partial_\sigma \mathbf{r}|$. Let $\mathrm{d}l = \xi_\sigma\,\mathrm{d}\sigma$ be a short length of the jth edge, with the energy $U_j\,\mathrm{d}l$. Attachment and detachment of adatoms causes the shift of $\eta = \eta_j$ by $\mathrm{d}\eta$ and the motion of the step edge along the local normal by $\mathrm{d}\rho = \xi_\eta \mathrm{d}\eta$; thus, the step energy $U_j \mathrm{d}l$ changes by $\mathrm{d}_\eta(U_j \mathrm{d}l)$, where $\mathrm{d}_\eta Q := Q|_{\eta+\mathrm{d}\eta} - Q|_\eta$. Hence, we obtain

$$\mu_j = \frac{\Omega}{a}\frac{\mathrm{d}_\eta(U_j \mathrm{d}l)}{\mathrm{d}\rho\,\mathrm{d}l} = \frac{\Omega}{a}\left[\xi_\eta^{-1}\partial_{\eta_i} U_i + U_i\,(\xi_\sigma \xi_\eta)^{-1}\partial_\eta \xi_\sigma\right] \qquad \eta = \eta_i. \tag{4}$$

Equation (4) is simplified via elementary differential geometry [25], by which $\partial_\perp \xi_\sigma = \kappa \xi_\sigma$ where κ is the curvature of the curve $\mathbf{r}(\eta, \sigma)$ with $\eta = $ const. and $\partial_\perp = \xi_\eta^{-1}\partial_\eta$; thus, $\partial_\eta \xi_\sigma = \kappa\,\xi_\sigma\,\xi_\eta$. The combination of the last relation regarding κ with (4) yields (3).

2.2. *Force dipole step interaction: a review*

A simple setting in homoepitaxy is a vicinal surface, which stems from cutting a crystal along a plane at a fixed, small angle with respect to a high-symmetry plane. The resulting interface consists of regularly spaced, atomic-height steps. This configuration is not as favorable energetically as a perfectly flat interface, so the atoms at the surface respond to their missing bonds by undergoing small displacements. We can expect such displacements to induce an effective elastic force between adjacent steps[9].

[8] Our definition of V in (1) and (2) is slightly different from that in [20].

[9] For a pictorial representation, consider the displacements calculated by atomistic simulations in [26].

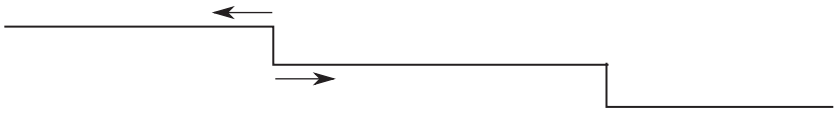

Figure 2. Schematic of a force dipole for a step by the MP model [2]. The dipole moment is along the step edge and normal to the cross-sectional plane.

Alternatively, picture a step as a defect on a continuous elastic surface. In order to maintain this defect against the natural tendency of the medium to flatten out, a pair of oppositely directed forces must be applied by the bulk of the crystal at distinct points of the step. Then, the step itself applies equal and opposite forces on the bulk of the crystal, as depicted in figure 2. This *force dipole* introduces strain in the vicinity of the step. The resulting strain field causes elastic interactions between steps by displacing the intervening atoms. Although the existence of a force dipole is inferred from considerations of a *continuous* elastic surface, such a dipole can also be justified while respecting the discrete nature of a real crystal surface, as argued, e.g., in [27]. For a discussion invoking *force quadrupoles of terrace adatoms* in homoepitaxy, see [4].

The question arises as to how the force dipole distribution near a step is calculated. A proposal involving a pair of forces oriented normal to the step edge in the high-symmetry plane, as shown in figure 2, first appeared in a paper by MP [2] and has since been used as a core model. This (MP) model has one free parameter, which is related to the strength of the force dipole[10].

Pimpinelli and Villain [15] adopt the MP model, positing that the elastic strain field stems from a line of force dipoles normal to the step. It is tempting to resort to electrostatics for the field of a force dipole. We do not pursue this analogy. It suffices to add that the scaling of the field strength as the inverse cube of the distance is common to both electric and elastic force dipoles [29, 30][11]. For an explicit calculation of the linear response of force dipoles, the reader may consult the appendices in [15]. The nature of the elastic force dipole interaction implies that steps of the same sign (i.e. steps either descending or ascending) exert *repulsive* forces on each other. The situation is different, and more delicate, with steps of opposite sign [6].

Extensive discussions on defect interactions for crystal surfaces can be found in [2, 15, 26, 27]. We appeal to the formulation in [15] to quantify the interaction energy of two force dipoles. In this work, the force dipole moments are defined as the mechanical moments, m_{bd}, stemming from forces $\mathbf{F}_k$ acting at points $\mathbf{R}_k$ [15]:

$$m_{bd} = \sum_k R_{k,b} F_{k,d} \quad (b, d = x, y, z),$$

where it is assumed that $\sum_k \mathbf{F}_k = 0$; (x, y, z) is a Cartesian coordinate system, z is the axis normal to the basal plane and $Q_{k,b}$ is the b component of the vector $\mathbf{Q}_k$. Assuming a cubic lattice, we adopt the formula [15]

$$m_{bd} = \delta_{bd}[(\delta_{bx} + \delta_{by})m + \delta_{bz} m_{zz}], \tag{5}$$

[10] Note in passing that Prévot and Croset [28] introduced a model of 'embedded dipoles', which describes the opposing forces by use of two free parameters rather than one. Accordingly, these authors were able to make predictions in close agreement with observed relaxations of atomistic simulations.

[11] Recall that the interaction energy of two electric dipoles with moments $\mathbf{p}_A$ and $\mathbf{p}_B$ at distance r_{AB} is [29] $W = \frac{1}{r_{AB}^3}[\mathbf{p}_A \cdot \mathbf{p}_B - 3(\mathbf{p}_A \cdot e_{AB})(e_{AB} \cdot \mathbf{p}_B)]$; e_{AB} is the unit vector pointing from A to B.

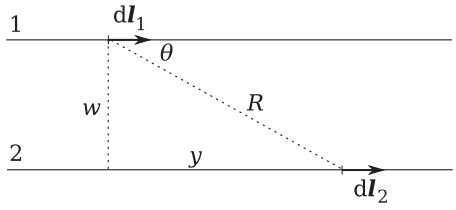

Figure 3. Geometry of straight steps.

where δ_{bd} is Kronecker's delta. The interaction energy of two such force dipoles with moments m and m' is calculated to be [15]

$$W_{\mathrm{int}}^{\mathrm{dip}} = \frac{1-\nu^2}{\pi Y R^3}\left[mm' - \frac{\nu}{1-\nu}(mm'_{zz} + m_{zz}m') + \left(\frac{\nu}{1-\nu}\right)^2 m_{zz}m'_{zz}\right], \tag{6}$$

where Y is Young's modulus, ν is the Poisson coefficient and R is the distance between the dipoles; typically, $1/5 \leqslant \nu < 1/2$ [31]. If the force dipoles lie in the high-symmetry plane as in the classic MP model (figure 2), then $m_{zz} = m'_{zz} = 0$. Alternatively, consider $|m_{zz}|, |m'_{zz}| \ll |m|$ and interpret our subsequent results as subject to corrections due to m_{zz} and m'_{zz}. So, we restrict attention to a truncated version of (6):

$$W_{\mathrm{int}}^{\mathrm{dip}} = \frac{1-\nu^2}{\pi Y R^3}\, mm'. \tag{7}$$

In the remainder of this paper, we invoke the symbol $\varpi = (1-\nu^2)/(\pi Y)$.

Equation (7) forms our starting point. The moments m and m' are expressed in a fixed coordinate system. If the step segments are not parallel, the product mm' in (7) must be appropriately replaced by the dot product of the respective vector moments.

3. 1D step geometries

In this section, we illustrate the application of (7) to simple geometries described in terms of a single spatial coordinate: straight steps and concentric circular steps. Lastly, we briefly consider a variant of the radial case with non-concentric circles.

3.1. Straight steps

Consider the case of two (infinite) straight steps shown in figure 3. The steps are aligned with the y-axis at a distance w (terrace width). To find the force dipole interaction energy per unit length of step 1, we fix the line element $\mathrm{d}\mathbf{l}_1$ and integrate over step 2, summing up the contributions of line elements $\mathrm{d}\mathbf{l}_2$. Let $\mathbf{R}$ be the vector along the line joining $\mathrm{d}\mathbf{l}_1$ and $\mathrm{d}\mathbf{l}_2$, θ be the angle formed by $\mathbf{R}$ and $\mathrm{d}\mathbf{l}_1$ and $R = |\mathbf{R}|$. Note the relations $R = w/\sin\theta$, $|\mathrm{d}\mathbf{l}_2| = \mathrm{d}l_2 = \mathrm{d}y = (w/\sin^2\theta)\,\mathrm{d}\theta$ where $0 \leqslant \theta \leqslant \pi$.

The dipole moments, m and m', are proportional to the lengths of the step segments, $\mathrm{d}l_1$ and $\mathrm{d}l_2$, with the proportionality constant P, the dipole moment per unit step length. Thus, the force dipole interaction energy per length of step 1 due to step 2 is

$$V_{\mathrm{int}} \equiv \frac{\mathrm{d}W_{\mathrm{int}}}{\mathrm{d}l_1} = \varpi\,\frac{P^2}{w^2}\int_0^\pi \sin\theta\,\mathrm{d}\theta = \varpi\,\frac{2P^2}{w^2}; \qquad \varpi = \frac{1-\nu^2}{\pi Y}. \tag{8}$$

Note that we replaced the symbol $W_{\mathrm{int}}^{\mathrm{dip}}$ of (7) by $\frac{\mathrm{d}^2 W_{\mathrm{int}}}{\mathrm{d}l_1\,\mathrm{d}l_2}$ and then integrated over $\mathrm{d}l_2$.

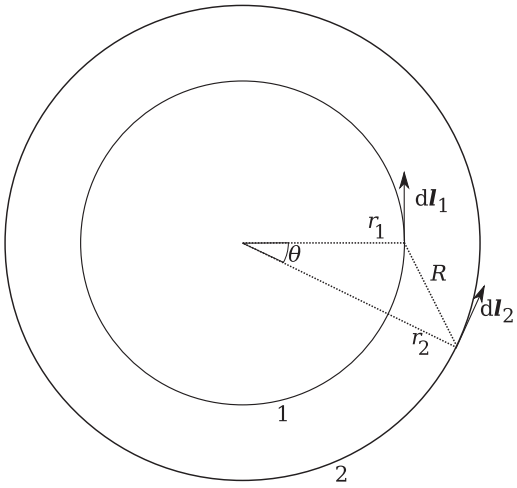

Figure 4. Geometry of concentric circular steps with radii r_1 and r_2.

3.2. Concentric circular steps

Next, we consider concentric circular steps, shown in figure 4. Our purpose is twofold. First, we aim to offer a streamline derivation of (2) for the interaction energy [16]. Second, we intend to clarify the role of a (assumed small) geometric parameter and demonstrate the use of the Mellin transform technique.

In figure 4, we fix our attention on the interaction between an (infinitesimal) element $d\mathbf{l}_1$ on the inner step (step 1) and the entire outer step (step 2). Recall formula (7), now written for two force dipoles on circles 1 and 2. The product mm' is proportional to $d\mathbf{l}_1 \cdot d\mathbf{l}_2$ where $d\mathbf{l}_j$ is an infinitesimal tangential vector along step j ($j = 1, 2$). By use of Cartesian coordinates (x, y), the dipoles are located at $(r_1, 0)$ and $(r_2 \cos\theta, r_2 \sin\theta)$.

If P is the force dipole moment per unit step length, the interaction energy per unit length of step 1 is[12]

$$V_{\text{int}} = \frac{dW_{\text{int}}}{dl_1} = \varpi\, P^2 \int_{-\pi}^{\pi} \frac{r_2 \cos\theta}{\left(r_1^2 + r_2^2 - 2r_1 r_2 \cos\theta\right)^{3/2}}\, d\theta. \tag{9}$$

This integral can be computed exactly in terms of elliptic integrals but the result does not reveal directly the dependence on r_1 and r_2 (see appendix A).

To render (9) amenable to approximation, we introduce a geometric parameter, δ, expressing the property that the terrace width, $r_2 - r_1$, is small compared to r_1 and r_2. Specifically, the independent parameters r_1 and r_2 of the radial setting are replaced by the parameters λ and δ, as outlined below.

- The parameter $\lambda/2$ expresses an appropriate average of r_1, r_2. For later algebraic convenience, define $\lambda = 2\sqrt{r_1 r_2}$. Note that for small $(r_2 - r_1)/r_1$ we have $\lambda \sim r_1 + r_2$.
- Define $\delta = (r_2 - r_1)/\lambda$ where $0 < \delta \ll 1$. Thus, we obtain $r_1(\delta, \lambda) = (\lambda/2)\left(\sqrt{1+\delta^2} - \delta\right)$ and $r_2(\delta, \lambda) = (\lambda/2)\left(\sqrt{1+\delta^2} + \delta\right)$.

[12] Because of rotational symmetry, the total interaction energy of steps 1 and 2 follows trivially.

Consequently, we compute (9) via the change of variable $s = \sin(\theta/2)$:

$$V_{\rm int}(\delta,\lambda) = \frac{4P^2\varpi r_2(\delta,\lambda)}{\lambda^3}\int_0^1 \frac{{\rm d}s}{\sqrt{1-s^2}}\frac{1-2s^2}{(s^2+\delta^2)^{3/2}} = \frac{4P^2\varpi r_2(\delta,\lambda)}{\lambda^3} I(\delta^2). \tag{10}$$

The task at hand is to evaluate $I(\delta^2)$, which diverges as $\delta \downarrow 0$.

3.2.1. Application of the Mellin transform. One may proceed by evaluating $I_{\rm int}(\delta^2)$ exactly in terms of complete elliptic integrals; see appendix A. Instead, we apply the Mellin transform in δ^2, which enables us to systematically identify the singularity in δ and derive directly an asymptotic expansion as $\delta \downarrow 0$. This procedure is applied to non-radial settings in section 4. For a review of the Mellin transform, see appendix B.

The Mellin-transformed integral of (10) reads

$$\hat{I}(\zeta) = \int_0^\infty I(\delta^2)(\delta^2)^{-\zeta}\,{\rm d}\delta^2 = \int_0^1 \frac{{\rm d}s(1-2s^2)}{\sqrt{1-s^2}}\left(\int_0^\infty \frac{(\delta^2)^{-\zeta}}{(s^2+\delta^2)^{3/2}}{\rm d}\delta^2\right),$$

by the interchange of the order of integrations. The integral for $\hat{I}(\zeta)$ converges for $-\frac{1}{2} < {\rm Re}\,\zeta < 0$ and can be evaluated in terms of the Gamma function [32]:

$$\hat{I}(\zeta) = \frac{\Gamma(1-\zeta)\Gamma(\zeta+\frac{1}{2})}{\Gamma(\frac{3}{2})}\int_0^1 {\rm d}(s^2)\frac{(s^2)^{-\zeta-1/2}}{\sqrt{1-s^2}}(1-2s^2) = -\frac{1}{2}\frac{\Gamma(1-\zeta)^2\,\Gamma(\frac{1}{2}+\zeta)}{\Gamma(\frac{1}{2}-\zeta)}\frac{\Gamma(\frac{1}{2})}{\Gamma(\frac{3}{2})}\left(\frac{1}{\zeta}+\frac{2}{\frac{1}{2}-\zeta}\right). \tag{11}$$

Recall that the sole singularities of $\Gamma(\omega)$ are simple poles at $\omega = -n = 0, -1, -2, \ldots$.

We invert (11) by summing over residues from poles that lie in the right half of the ζ-plane and are closest to the fundamental strip. So, we write

$$I(\delta^2) = \frac{1}{2\pi{\rm i}}\int_{\tau-{\rm i}\infty}^{\tau+{\rm i}\infty}(\delta^2)^{\zeta-1}\hat{I}(\zeta)\,{\rm d}\zeta, \qquad -\frac{1}{2} < \tau < 0, \tag{12}$$

by definition 2 of appendix B. By shifting the contour to the right, the *leading-order term* in (12) comes from the residue at $\zeta = 0$. Thus, we approximate [32]

$$(\delta^2)^{\zeta-1}\hat{I}(\zeta) \sim -\frac{1}{2\delta^2}\frac{\Gamma(\frac{1}{2})}{\Gamma(\frac{3}{2})}\frac{1}{\zeta} = -\frac{1}{\delta^2}\frac{1}{\zeta} \qquad \text{as} \quad \zeta \to 0.$$

The respective residue at $\zeta = 0$ is $-1/\delta^2$. Thus, by (12) we find

$$I(\delta^2) \sim \frac{1}{\delta^2} \;\Rightarrow\; V_{\rm int}(\delta,\lambda) \sim \frac{4\varpi P^2 r_2(\delta,\lambda)}{\lambda^3\delta^2} \qquad \text{as} \quad \delta \downarrow 0. \tag{13}$$

To leading order in δ^2, the force dipole interaction energy per unit length is

$$V_{\rm int} \sim \frac{\varpi}{2}\sqrt{\frac{r_2}{r_1}}\left(\frac{2P}{r_2-r_1}\right)^2 \sim \frac{\varpi}{2}\left(\frac{2r_2}{r_1+r_2}\right)\left(\frac{2P}{r_2-r_1}\right)^2, \qquad \frac{r_2-r_1}{r_1+r_2} \ll 1, \tag{14}$$

where we used $\lambda = 2\sqrt{r_1 r_2} \sim r_1 + r_2$ and $\delta = (r_2 - r_1)/\lambda$. Formula (14) is in agreement with (2) via the substitution $2P^2\varpi = a^2 g$ [16, 19]. By setting $r_2 - r_1 = w$ fixed with $r_1 \gg w$ and $r_2 = r_1 + w$ so that $\frac{2r_2}{r_1+r_2} \sim 1$, we recover the straight-step energy (8).

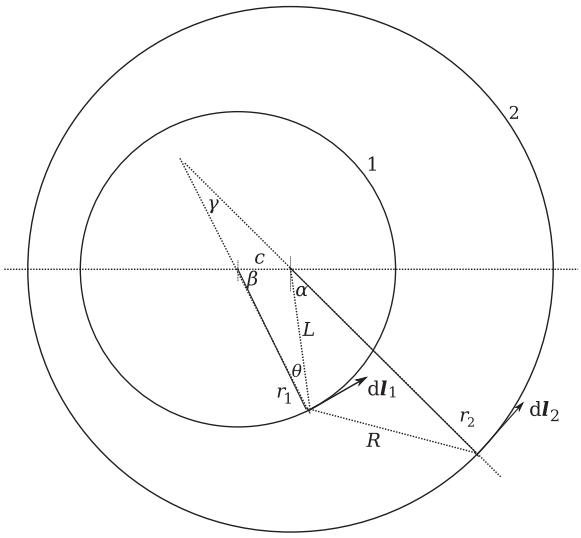

Figure 5. Geometry of non-concentric circular steps of radii r_1 and r_2.

In this vein, corrections to (14) originate from residues at the poles $\zeta = 1, 2, \ldots$ of $\hat{I}(\zeta)(\delta^2)^{\zeta-1}$. In particular, the residue at $\zeta = 1$ is found via expansions in $\tilde{\zeta} = 1 - \zeta$. Using the recursive relation $\omega\Gamma(\omega) = \Gamma(\omega + 1)$ [32] where necessary, we have

$$\hat{I}(\zeta) \sim \frac{1}{4}\left[-\frac{3}{\tilde{\zeta}^2} - \frac{6\psi(1) - 3\psi(3/2) - 3\psi(-1/2) + 7}{\tilde{\zeta}}\right] \qquad \text{as } \tilde{\zeta} \to 0,$$

where $\psi(\omega) = \frac{\mathrm{d}}{\mathrm{d}\omega}\ln\Gamma(\omega)$ [32]. Thus, $(\delta^2)^{\zeta-1}\hat{I}(\zeta)$ has the residue $\frac{1}{4}\left(-3\ln\frac{16}{\delta^2} + 5\right)$ at $\zeta = 1$. Accordingly, we obtain a *logarithmic correction* for V_{int}:

$$V_{\text{int}} \sim \varpi P^2 \sqrt{\frac{r_2}{r_1}}\left\{\frac{2}{(r_2 - r_1)^2} - \frac{1}{8}\frac{1}{r_1 r_2}\left[3\ln\left(\frac{64 r_1 r_2}{(r_2 - r_1)^2}\right) - 5\right]\right\}. \tag{15}$$

Further corrections in this context may be questionable, since these may be comparable in magnitude to terms omitted from our starting point, equation (6).

3.3. Non-concentric circular steps

In this section, we briefly consider two circular steps of different centers and show that the computation of the force dipole interaction energy is essentially unaltered in comparison to section 3.2 (radial case).

The geometry is depicted in figure 5. Let the circle radii be r_1 and r_2 and their centers be at a distance c on the x-axis. The centers and the fixed point of interest on the inner circle (step 1) form a triangle of sides with lengths c, r_1 and L (a dependent parameter). The dipole $\mathbf{dl}_1$ on step 1 is located at angle β with the x-axis[13]. The dipole $\mathbf{dl}_2$ on step 2 is located at angle α with the side of length L. We also define the auxiliary angles γ and θ, and the distance R between the two dipoles. Note that $\alpha = \theta + \gamma$, $\cos\gamma = [1 - (c\sin\beta/L)^2]^{1/2}\cos\alpha + (c/L)\sin\alpha\sin\beta$,

[13] For the interaction energy per unit length, it suffices to take $\mathbf{dl}_1$ on a fixed (say, the y-) axis. Here, we choose to also give a formula for the total energy, so β is needed to parameterize the position of $\mathbf{dl}_1$.

$R^2 = L^2 + r_2^2 - 2Lr_2\cos\alpha$ and $L^2 = r_1^2 + c^2 - 2r_1 c\cos\beta$. We compute the dipole interaction energy per step length

$$V_{\text{int}}^{\text{nc}} = \frac{\mathrm{d}W_{\text{int}}}{\mathrm{d}l_1} = \varpi P^2 r_2 \int_{-\pi}^{\pi} \frac{\cos\alpha\sqrt{1-\left(\frac{c}{L}\sin\beta\right)^2} + \frac{c}{L}\sin\alpha\sin\beta}{(L^2 + r_2^2 - 2r_2 L\cos\alpha)^{3/2}}\,\mathrm{d}\alpha.$$

By $s = \sin(\alpha/2)$, this is recast to a form analogous to the radial case (section 3.2):

$$V_{\text{int}}^{\text{nc}} = \frac{4\varpi P^2 r_2(\delta,\lambda)}{\lambda^3}\sqrt{1-\left(\frac{c}{L(\delta,\lambda)}\sin\beta\right)^2}\, I(\delta^2), \quad \delta = \frac{r_2 - L}{\lambda}, \tag{16}$$

where $\lambda^2 := 4r_2 L$. Thus, for fixed β, the independent parameters here are δ, λ and c, with $L = (\lambda/2)(\sqrt{1+\delta^2} - \delta)$, $r_2 = (\lambda/2)(\sqrt{1+\delta^2} + \delta)$ and $I(\delta^2)$ defined by (10).

Hence, by (13), the leading-order approximation for the elastic (force dipole) interaction energy per unit length of step 1 is

$$V_{\text{int}}^{\text{nc}} = \frac{\mathrm{d}W_{\text{int}}^{\text{nc}}}{\mathrm{d}l_1} \sim \frac{\varpi}{2}\sqrt{\frac{r_2}{L}}\sqrt{1-\left(\frac{c}{L}\sin\beta\right)^2}\left(\frac{2P}{r_2 - L}\right)^2, \tag{17}$$

provided $r_2 - L \ll \sqrt{r_2 L}$. Formula (17) reduces to approximation (14) of the radial case as $c \to 0$. Correction terms follow from the higher order terms in the expansion for $I(\delta^2)$; see section 3.2.

Remark 1. By (17), the *total* force dipole interaction energy of steps 1 and 2 is

$$W_{\text{int}}^{\text{nc}} \sim \varpi r_1 \int_0^{\pi} \sqrt{\frac{r_2}{L(\beta)}}\sqrt{1-\left(\frac{c}{L(\beta)}\sin\beta\right)^2}\left(\frac{2P}{r_2 - L(\beta)}\right)^2 \mathrm{d}\beta,$$

where by abusing notation we write $L(\beta) = L(\delta(\beta), \lambda(\beta))$. Now consider variations in c of this energy (perturbing the radial setting, $c = 0$) with $0 < c \ll r_2 - r_1 \ll r_1, r_2$. We find that the interaction energy of non-concentric circular steps exceeds the energy, $W_{\text{int}}^{\text{cir}}$, of the radial case by $\Delta W_{\text{int}} = W_{\text{int}}^{\text{nc}} - W_{\text{int}}^{\text{cir}} \sim 6\pi\varpi P^2\sqrt{r_1 r_2}\,\frac{c^2}{(r_2 - r_1)^4}$. So, the force dipole interaction disfavors relative displacements (offsets) of the circle centers.

4. Perturbation of concentric circular step profiles

In this section we address the computation of the force dipole interaction energy, V_{int}, of smooth step profiles that form perturbations of concentric circles. The steps are represented in a polar coordinate system (with the same center). An assumption is that the polar coordinates r_1 and r_2 differ by a sufficiently small length, by analogy with the radial case (section 3.2), and are sufficiently slowly varying. From the viewpoint of our analysis, which employs the Mellin transform, the requisite integrals are directly amenable to approximations if $|r_1 - r_2|$ is small compared to r_1 and r_2, and derivatives of r_1 and r_2 in the angle variables are small compared to $|r_1 - r_2|$.

The geometry is shown in figure 6. The system consists of (i) step profile 1 with the polar graph $(r_1(\alpha), \alpha)$, and (ii) step 2 described by $(r_2(\beta), \beta)$. Here, we parameterize step 1 by α since we will eventually compute the total force dipole interaction energy of steps 1 and 2 (see remark 2); $r_j(\theta)$ ($j = 1, 2$ and $\theta = \alpha, \beta$) are smooth, $-\pi < \theta \leqslant \pi$. If the unit vectors of the basal xy plane are e_x and e_y, the local orientation of a force dipole on step profile j is $\mathrm{d}\mathbf{l}_j = (\dot{r}_j\cos\theta - r_j\sin\theta)e_x + (\dot{r}_j\sin\theta + r_j\cos\theta)e_y$ where the dot on top of r_j denotes differentiation in the angle (α or β) variable.

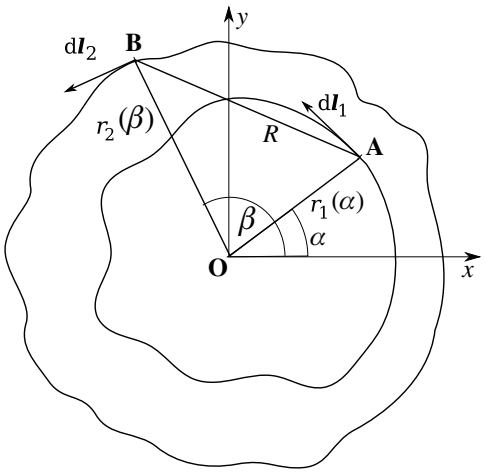

Figure 6. Geometry of step profiles forming perturbations of concentric circles in the polar coordinate system of center O.

Fix α and consider a force dipole along $d\mathbf{l}_1$ at a distance R from a dipole at β on step 2. By analogy with the radial case (section 3.2) we give the following definitions.

- Set $\lambda(\alpha) = 2\sqrt{r_1(\alpha)r_2(\alpha)}$ for $-\pi < \alpha \leqslant \pi$.
- Define $\delta(\alpha) = [r_2(\alpha) - r_1(\alpha)]/\lambda(\alpha)$ and assume $0 < \delta \ll 1$ for all α.

Accordingly, we write $r_2(\beta) = r_1(\alpha) + \rho(\alpha)[1 + \tilde{r}_2(\beta;\alpha)]$ where $\rho(\alpha) = r_2(\alpha) - r_1(\alpha) = \lambda\delta$ and $\tilde{r}_2(\beta;\alpha) = [r_2(\beta) - r_2(\alpha)]/[r_2(\alpha) - r_1(\alpha)]$ signifies the breaking of rotational symmetry. For later algebraic convenience, let $\tilde{r}_2(\beta;\alpha) =: s\bar{r}(s;\alpha)$ where $s = \sin\left(\frac{\beta-\alpha}{2}\right)$. Note that $\rho\bar{r}(0) = 2\dot{r}_2$ and $\rho\bar{r}'(0) = 2\ddot{r}_2$ at α; and $d\mathbf{l}_1 \cdot d\mathbf{l}_2 = (\dot{r}_1\dot{r}_2 + r_1r_2)(1 - 2s^2) + 2(\dot{r}_1r_2 - r_1\dot{r}_2)s\sqrt{1-s^2}$, where the prime (dot) denotes differentiation in s (β or α). We assume that $\bar{r}(s;\alpha)$ and its derivatives in s are small for all α.

By suppression of α, the distance R is now written as $R(s;\delta,\lambda)^2 = \lambda^2\mathcal{Q}(s;\delta^2)$ where $\mathcal{Q} = \mathcal{Q}_0 + \bar{r}\,\varsigma(\delta)\,\delta\,s^3$, with

$$\mathcal{Q}_0(s;\delta^2) = s^2 + \delta^2[1 + sA(s)], \quad A(s) = \bar{r}(s)[2 + s\bar{r}(s)], \tag{18}$$

and $\varsigma(\delta) = 2(\sqrt{1+\delta^2} - \delta)$. Assume that $\bar{r}(s;\alpha) \neq 0$ for definiteness. The computation of the interaction energy per unit length involves integration in s ($-1 \leqslant s \leqslant 1$).

Before we compute the desired energy, we argue why we can keep only $\mathcal{Q}_0$ in the denominator of the requisite integrals. The relevant factor is split as

$$\frac{1}{R^3} = \frac{1}{\lambda^3}\left\{\frac{1}{\mathcal{Q}_0^{3/2}} - \delta\frac{\bar{r}\varsigma s^3[2\mathcal{Q}_0 + \mathcal{Q}_0^{1/2}(\mathcal{Q}_0 + \bar{r}\varsigma\delta s^3)^{1/2} + \bar{r}\varsigma\delta s^3]}{\mathcal{Q}_0^{3/2}(\mathcal{Q}_0 + \bar{r}\varsigma\delta s^3)^{3/2}[(\mathcal{Q}_0 + \bar{r}\varsigma\delta s^3)^{1/2} + \mathcal{Q}_0^{1/2}]}\right\}.$$

The second term on the right-hand side behaves as $(s|s|)^{-1}\delta$ if $\delta \downarrow 0$. As indicated in appendix C (through evaluation of germane integrals by the Mellin transform), the corresponding integral would be of the order of $\delta\ln(1/\delta^2)$ or smaller. Thus, we can neglect the term $\bar{r}\,\varsigma(\delta)\,\delta\,s^3$ in $\mathcal{Q}$ *provided we restrict attention up to (bounded) terms* $\mathcal{O}(1)$ in asymptotic expansions in δ of the requisite integrals $\int_{-1}^{1}\frac{s^l f(s)}{\mathcal{Q}_0(s)^{3/2}}\,ds$ (see (20)).

We now proceed with the calculation of the force dipole interaction energy, $V_{\rm int}$, per unit length of step 1, for the fixed angle α. After some algebra, we obtain the formula

$$V_{\rm int}(\alpha) = \frac{P^2\varpi}{\ell_1}\int_{-\pi}^{\pi}\frac{(\dot r_1\dot r_2 + r_1 r_2)\cos(\beta-\alpha) - (\dot r_1 r_2 - r_1\dot r_2)\sin(\beta-\alpha)}{R^3}\mathrm{d}\beta$$
$$\sim \frac{2\varpi P^2}{\ell_1\lambda^3}\Big\{r_1(r_1+\rho)I_{00} + \frac{1}{2}\dot r_1\rho I_{01} + 2\rho r_1 I_{10} - 2\dot r_1(r_1+\rho)I_{11}$$
$$+\frac{1}{2}\dot r_1\rho I_{12} + \rho r_1 I_{20} - 2(r_1+\rho)r_1 I_{21} - 3\dot r_1\rho I_{22}$$
$$-3\rho r_1 I_{30} - \dot r_1\rho I_{31} - \rho r_1 I_{40}\Big\},\ \ell_1(\alpha) = \sqrt{r_1(\alpha)^2 + \dot r_1(\alpha)^2}, \qquad (19)$$

where the integrals I_{lk} are classified according to the power l of s appearing explicitly in each numerator. These integrals are defined by

$$I_{lk}(\delta^2) = \int_{-1}^{1}\frac{\mathrm{d}s}{\sqrt{1-s^2}}\frac{s^l f_{lk}(s)}{\mathcal{Q}_0(s;\delta^2)^{3/2}}, \qquad l = 0,\ 1,\ 2,\ 3,\ 4, \qquad (20)$$

$$f_{00}(s) = 1, \quad f_{01}(s) = \sqrt{1-s^2}\bar r(s) \quad (k = 0, 1),$$
$$f_{10}(s) = \bar r(s), \quad f_{11}(s) = \sqrt{1-s^2}, \quad f_{12}(s) = \sqrt{1-s^2}\bar r'(s),$$
$$f_{20}(s) = \bar r'(s), \quad f_{21}(s) = 1, \quad f_{22}(s) = \sqrt{1-s^2}\bar r(s),$$
$$f_{30}(s) = \bar r(s), \quad f_{31}(s) = \sqrt{1-s^2}\bar r'(s), \quad f_{40}(s) = \bar r'(s).$$

As $\delta^2 \downarrow 0$, the most singular integrals are $I_{0k}(\delta^2)$ $(k = 0,\ 1)$.

In appendix C, the above integrals are approximated for small δ^2 ($\delta^2 \ll 1$) by use of the Mellin transform. The main idea is to single out the contributions of the underlying divergences (as $\delta^2 \downarrow 0$) in the form of appropriate residues of a complex-valued function. Our results, up to (and including) logarithmic corrections, are summarized as follows:

$$I_{00}(\delta^2) \sim \frac{2}{\delta^2} + \frac{1}{2}\ln\frac{16}{\delta^2} - \frac{1}{2}[2A'(0) - A(0)^2 + 3], \qquad (21)$$

$$I_{01}(\delta^2) \sim \frac{2\bar r(0)}{\delta^2} + \frac{1}{2}\bar r''(0)\ln\frac{16}{\delta^2} + \frac{1}{2}\big\{\bar r(0)[A(0)^2 - 1]$$
$$-2\bar r''(0) - 2[\bar r'(0)A(0) + \bar r(0)A'(0)]\big\}, \qquad (22)$$

$$I_{10}(\delta^2) \sim \bar r'(0)\left(\ln\frac{16}{\delta^2} - 2\right) + \bar r(0)A(0) + \mathcal{C}_{10}, \qquad (23)$$

$$I_{11}(\delta^2) \sim A(0), \quad I_{12}(\delta^2) \sim \bar r''(0)\left(\ln\frac{16}{\delta^2} - 2\right) + \bar r'(0)A(0) + \mathcal{C}_{12}, \qquad (24)$$

$$I_{20}(\delta^2) \sim \bar r'(0)\left(\ln\frac{16}{\delta^2} - 2\right) + \mathcal{C}_{20}, \quad I_{21}(\delta^2) \sim \ln\frac{16}{\delta^2} - 2, \qquad (25)$$

$$I_{22}(\delta^2) \sim \bar r(0)\left(\ln\frac{16}{\delta^2} - 2\right) + \mathcal{C}_{22}, \qquad (26)$$

$$I_{30}(\delta^2) \sim \mathcal{C}_{30} = \int_{-1}^{1} \frac{\mathrm{d}s}{\sqrt{1-s^2}}\, \bar{r}(s)\,\mathrm{sgn}(s), \quad I_{31}(\delta^2) \sim 2[\bar{r}(1) - \bar{r}(0)], \tag{27}$$

$$I_{40}(\delta^2) \sim \mathcal{C}_4 = \int_{-1}^{1} \frac{\mathrm{d}s}{\sqrt{1-s^2}}\, \bar{r}'(s)\,|s|, \tag{28}$$

where $\mathrm{sgn}(s) = -1$ if $s < 0$ and $\mathrm{sgn}(s) = 1$ if $s > 0$, and

$$\mathcal{C}_{10} = \int_{-1}^{1} \frac{\mathrm{d}s}{\sqrt{1-s^2}} \left[\frac{\bar{r}(s) - \bar{r}(0)}{s} - \bar{r}'(0) \right] |s|^{-1}, \tag{29}$$

$$\mathcal{C}_{12} = \int_{-1}^{1} \frac{\mathrm{d}s}{\sqrt{1-s^2}} \left[\frac{\sqrt{1-s^2}\,\bar{r}'(s) - \bar{r}'(0)}{s} - \bar{r}''(0) \right] |s|^{-1}, \tag{30}$$

$$\mathcal{C}_{20} = \int_{-1}^{1} \frac{\mathrm{d}s}{\sqrt{1-s^2}}\, [\bar{r}'(s) - \bar{r}'(0)]\,|s|^{-1}, \tag{31}$$

$$\mathcal{C}_{22} = \int_{-1}^{1} \frac{\mathrm{d}s}{\sqrt{1-s^2}} \left[\sqrt{1-s^2}\,\bar{r}(s) - \bar{r}(0) \right] |s|^{-1}, \tag{32}$$

$$A(0) = 2\bar{r}(0), \quad A'(0) = 2\bar{r}'(0) + \bar{r}(0)^2. \tag{33}$$

The corresponding expansion for $V_{\mathrm{int}} = \mathrm{d}W_{\mathrm{int}}/\mathrm{d}l_1$ follows from (19)–(28):

$$V_{\mathrm{int}}(\alpha) \sim \frac{2\varpi P^2}{\lambda^3} \frac{r_1}{\ell_1} (r_1 + \rho) \left\{ \left[2 + \frac{\dot{r}_1}{r_1} \frac{\rho}{r_1 + \rho} \bar{r}(0) \right] \frac{1}{\delta^2} \right.$$
$$\left. + 3 \left[-\frac{1}{2} + \frac{\rho}{r_1 + \rho} \bar{r}'(0) + \frac{\dot{r}_1}{r_1} \frac{\rho}{r_1 + \rho} \left(\frac{\bar{r}''(0)}{4} - \bar{r}(0) \right) \right] \ln \frac{16}{\delta^2} + \frac{5}{2} - 2\bar{r}'(0) \right\}. \tag{34}$$

Here, we neglect terms of the order of $\rho\bar{r}$ or smaller inside the curly brackets. Recall that r_1, ρ, λ, δ, ℓ_1 and $\bar{r}(0) = \bar{r}(s = 0)$ are evaluated at an angle α; $\rho + r_1 = r_2$. For $\bar{r}(s; \alpha) \equiv 0$ (radial case), (34) reduces to formula (15). For a non-circular step 2, the logarithmic correction in (34) involves the curvature of step 2 at α. We expect that higher order terms in δ for V_{int} (properly computed) contain higher derivatives of $\bar{r}(s)$.

The leading-order term in (34) is consistent with the geometric factor based on local coordinates in [22]. This is not surprising since the present geometry is a (regular) perturbation of concentric circles.

We reiterate that the magnitude of corrections to (34) relative to terms omitted in (6) is not known *a priori*. Adding corrections from other residues here might not be enough to ensure overall accuracy. Estimating cross-terms in (6) that stem from dipole moments perpendicular to the basal plane lies beyond our present scope.

Remark 2. It is of interest to mention an implication of (34) regarding energy variations of modulated closed step profiles. In the spirit of [4], consider the steps represented by

$$r_1(\alpha) = \mathcal{R}_1[1 + \epsilon \sin(n\alpha)], \quad r_2(\alpha) = \mathcal{R}_2[1 + \epsilon \sin(n\alpha + \vartheta)],$$

where $0 < \epsilon \ll \delta := (\mathcal{R}_2 - \mathcal{R}_1)/\sqrt{\mathcal{R}_1\mathcal{R}_2} \ll 1$, n is a positive integer and ϑ is a given phase shift, $0 \leqslant \vartheta \leqslant \pi$. By (34) we compute the force dipole interaction energy, $V_{\mathrm{int}} = \mathrm{d}W_{\mathrm{int}}/\mathrm{d}l_1$, per unit length of step 1, and thereby determine the total interaction energy

$W_{\rm int} = \int_{-\pi}^{\pi} V_{\rm int}(\alpha)\, \ell_1(\alpha) \mathrm{d}\alpha$ of steps 1 and 2. By subtracting the energy of the radial case (where $\epsilon = 0$), we find the leading-order *excess energy*

$$\Delta W_{\rm int} \sim \frac{\pi P^2 \varpi}{4} \frac{\sqrt{\mathcal{R}_1 \mathcal{R}_2}}{(\mathcal{R}_2 - \mathcal{R}_1)^2} \epsilon^2 \left[14 - 6\cos\vartheta + 48 \frac{\mathcal{R}_1 \mathcal{R}_2}{(\mathcal{R}_2 - \mathcal{R}_1)^2} (1 - \cos\vartheta) + 8n^2 \cos\vartheta \right]. \tag{35}$$

Here, we neglected terms of the order of ϵ^3 or smaller, as well as logarithmic and higher order corrections in δ. This calculation indicates that the force dipole interaction does not favor step modulations unless the wavenumber n is large enough, $n \geqslant \mathcal{O}(\delta^{-1})$. Because of limitations due to the nature of our asymptotics, which treats n as a fixed parameter, we do not discuss this case of large n here.

5. Conclusion

We began this investigation in an attempt to verify, and possibly improve, a previously used formula for the force dipole interaction energy between two concentric circular steps in homoepitaxy. To this end, we applied the Mellin transform of the requisite interval with respect to a parameter expressing the relative magnitude of the interstep distance and step radii. This technique singles out the most important contributions to integration over the step circumference in the form of residues of the transformed integral. Our derivation led to a logarithmic correction to the previous formula.

We point out that the Mellin transform is not the only tool for evaluating asymptotically integrals for elastic energies. A direct recourse to elliptic integrals is another route, as discussed in appendix A. The Mellin transform reveals elegantly a connection of divergences of requisite integrals to singularities in the complex plane.

We extended the calculation of the force dipole interaction energy to a class of smooth 2D steps, which form perturbations of concentric circles. The leading-order term is consistent with physical intuition: the energy per unit length decays as the inverse square of step separation, as measured along the appropriate *local normal*. This property was invoked by Weeks, Liu and Jeong [10] for perturbations of straight steps.

Our setting also differs from the geometry of Houchmandzadeh and Misbah [4], who study perturbations of straight steps. In the spirit of these authors' work, we studied variations of the force dipole interaction energy caused by small-amplitude modulations of concentric circular steps. We find that modulations of such steps are not preferred energetically (in the force dipole model) for a fixed wavenumber. The possibility of creating energetically favorable modulations by choice of the phase shift for large wavenumber is left open. Our asymptotics does not treat this case. We expect that the step line tension will dominate over the elastic contribution, causing an overall stabilizing effect (as discussed extensively in [4]).

Previous numerical studies of the step flow with circular steps [17, 19] made use of the interaction energy formula from [16], which we now understand to be valid when step separations are sufficiently small compared to the step radii ($\delta^2 \ll 1$ in our notation). A more precise regime of validity of this formula should stem from considering limitations of continuum elasticity as well; for example, the starting force dipole formula becomes inadequate if the interstep distance becomes comparable to a few atomic lengths [26].

Our analysis has limitations. We did not address contributions of dipole moments perpendicular to the basal plane. We did not compute the contribution of force monopole step interactions, which arise in heteroepitaxy [4]. Our goal was to demonstrate the use of the Mellin transform in simple yet nontrivial geometries. Other elastic step energies amenable to the Mellin transform are the subject of work in progress.

Acknowledgments

The authors are indebted to T L Einstein for discussions. John Quah's research was supported by NSF-MRSEC under grant DMR-0520471 during the spring of 2009. The work of Li Peng Liang was supported by the NSF-MRSEC REU via grant DMR-0520471 at the University of Maryland. Dionisios Margetis's research was supported by NSF under grant DMS-0847587.

Appendix A. On elliptic integrals

In this appendix, we compute the integral $V_{\rm int}(\delta^2)$ of the radial case, equation (10), in terms of complete elliptic integrals [33].

Using (10), we express $V_{\rm int}(\delta^2)$ as

$$V_{\rm int}(\delta^2) = \frac{4\varpi P^2 r_2}{\lambda^3}\left[-2(2\delta^2+1)\frac{\mathrm{d}}{\mathrm{d}(\delta^2)} - 2\right] I_{\rm c}(\delta^2), \tag{A.1}$$

where

$$I_{\rm c}(\delta^2) = \int_0^1 \frac{\mathrm{d}s}{\sqrt{1-s^2}}\,\frac{1}{\sqrt{s^2+\delta^2}}. \tag{A.2}$$

With $s = \cos\theta$ in (A.2), we find

$$I_{\rm c}(\delta^2) = \int_0^{\pi/2} \frac{\mathrm{d}\theta}{\sqrt{\delta^2+1-\sin^2\theta}} = \frac{1}{\sqrt{1+\delta^2}}\,\mathbb{K}\big(1/\sqrt{1+\delta^2}\big), \tag{A.3}$$

where $\mathbb{K}(\chi) = \int_0^{\pi/2} \mathrm{d}\theta\,(1-\chi^2\sin^2\theta)^{-1/2}$ is the complete elliptic integral of the first kind [33]. Thus, by (A.1) and $\chi = \chi(\delta^2) = (1+\delta^2)^{-1/2}$, we obtain

$$V_{\rm int}(\delta^2) = \frac{4\varpi P^2 r_2(\delta,\lambda)}{\lambda^3}\,\chi(\delta^2)\left[\frac{2-\chi(\delta^2)^2}{1-\chi(\delta^2)^2}\mathbb{E}(\chi(\delta^2)) - 2\mathbb{K}(\chi(\delta^2))\right]; \tag{A.4}$$

$\mathbb{E}(\chi) = \int_0^{\pi/2}\sqrt{1-\chi^2\sin^2\theta}\,\mathrm{d}\theta$ is the complete elliptic integral of the second kind [33].

This result is compatible with the asymptotic expansion of section 3.2. In particular, by expanding $(1+\delta^2)^{-1/2}$ about $\delta = 0$ and using an expansion of $\mathbb{K}(\chi)$ about $\chi = 1$ [33], we recover $I_{\rm c} \sim \ln(16/\delta^2)$ and the assorted correction terms as $\delta \downarrow 0$.

Appendix B. Review of the Mellin transform

In this appendix, we review elements of the Mellin integral transform. For a more thorough discussion including other applications, the reader may consult, e.g., [13, 14, 34–36]. We include only technical elements that serve our present purposes.

Definition 1. *The Mellin transform of* $F(x) : \mathbb{R}_+ \to \mathbb{R}$ *(*$\mathbb{R}$*: set of reals) is defined as*

$$\hat{F}(\zeta) = \int_0^\infty F(x)x^{-\zeta}\,\mathrm{d}x, \tag{B.1}$$

where ζ *lies in some vertical strip,* $\mathbb{S}_0$*, of the complex plane so that the integral converges.*

Note that, once defined via (B.1) for $\zeta \in \mathbb{S}_0$, the function $\hat{F}(\zeta)$ can in principle be continued analytically to the whole complex plane, $\mathbb{C}$.

Definition 2. *The inverse Mellin transform of* $\hat{F}(\zeta) : \mathbb{C} \to \mathbb{C}$ *is defined by*

$$(\hat{F})^{\vee}(x) = \frac{1}{2\pi \mathrm{i}} \int_{\tau-\mathrm{i}\infty}^{\tau+\mathrm{i}\infty} \hat{F}(\zeta) x^{\zeta-1} \, \mathrm{d}\zeta \qquad (i^2 = -1), \tag{B.2}$$

where, for appropriate τ*, the contour of integration must lie in* $\mathbb{S}_0 \subset \mathbb{C}$*.*

Under reasonably general assumptions on $F(x)$, we henceforth take $F(x) = (\hat{F})^{\vee}(x)$ (almost everywhere). In the following, we motivate formulas (B.1) and (B.2) with recourse to a (presumably more familiar) variant of the Fourier transform.

For a function $f : \mathbb{R} \to \mathbb{R}$, the *two-sided Laplace transform* is

$$\mathcal{L}(f)(\sigma) = \int_{-\infty}^{\infty} f(t) \mathrm{e}^{-\sigma t} \, \mathrm{d}t, \tag{B.3}$$

which follows from the Fourier transform [34]. By reasonably general conditions, f is recovered from $\mathcal{L}(f)$ via the inversion formula

$$f(t) = \frac{1}{2\pi \mathrm{i}} \int_{\gamma-\mathrm{i}\infty}^{\gamma+\mathrm{i}\infty} \mathcal{L}(f)(\sigma) \mathrm{e}^{\sigma t} \, \mathrm{d}\sigma, \tag{B.4}$$

where the integration path lies in the region of convergence of the integral for $\mathcal{L}(f)(\sigma)$.

The Mellin transform ensues from (B.3) by the change of variable $x = \mathrm{e}^t$:

$$\mathcal{L}(f)(\sigma) = \int_0^{\infty} f(\ln x) x^{-\sigma-1} \, \mathrm{d}x, \tag{B.5}$$

which leads to (B.1) via the definitions $F(x) = f(\ln x)$, $\zeta = \sigma + 1$ and $\hat{F}(\zeta) = \mathcal{L}(f)(\zeta - 1)$. The inverse Mellin transform (B.2) with $(\hat{F})^{\vee} = F$ follows from (B.4).

We add a note on convergence. For arbitrary yet fixed $c > 0$, split integral (B.1) as

$$\hat{F}(\zeta) = \left(\int_0^c + \int_c^{\infty} \right) F(x) x^{-\zeta} \, \mathrm{d}x, \tag{B.6}$$

and assume that $F(x)$ is summable on any finite $(c_1, c_2) \subset (0, \infty)$ where $c_1 > 0$, $F(x) = \mathcal{O}(x^{p_2-1})$ as $x \downarrow 0$ and $F(x) = \mathcal{O}(x^{p_1-1})$ as $x \to \infty$. The first integral converges provided $\mathrm{Re}\,\zeta < p_2$, while the second one converges if $p_1 < \mathrm{Re}\,\zeta$. Thus, if $p_1 < p_2$, $\hat{F}(\zeta)$ is originally defined (as a convergent integral) in the *fundamental strip* $p_1 < \mathrm{Re}\,\zeta < p_2$.

Appendix C. Asymptotics for integrals of a non-circular step

In this appendix, we evaluate approximately integrals of the form

$$I_l(\delta^2) = \int_{-1}^{1} \frac{\mathrm{d}s}{\sqrt{1-s^2}} \frac{s^l f(s)}{\mathcal{Q}_0(s;\delta^2)^{3/2}}, \qquad \delta^2 \ll 1, \tag{C.1}$$

where $\mathcal{Q}_0$ is defined in (18), assuming that $f(s)$ is smooth in $(-1,1)$ with $f(0) \neq 0$, and $l = 0$–4. This type of integrals is needed in section 4, cf (20). We resort to the Mellin transform $\hat{I}_l(\zeta)$. Each $\hat{I}_l(\zeta)$ is a meromorphic function and can be written as a Laurent series in the vicinity of each pole. By starting with the definition of the Mellin transform in the fundamental strip, we derive terms of the Laurent series by *analytic continuation*. So, the respective residues are computed to yield an asymptotic expansion in δ with terms containing details of the step curve.

Integral I_0. This is the most singular integral. We compute

$$\hat{I}_0(\zeta) = \frac{\Gamma(1-\zeta)\,\Gamma\left(\frac{1}{2}+\zeta\right)}{\Gamma\left(\frac{3}{2}\right)} \int_{-1}^{1} \frac{\mathrm{d}s}{\sqrt{1-s^2}} f(s)[1+sA(s)]^{\zeta-1} (s^2)^{-\zeta-1/2}, \tag{C.2}$$

with the fundamental strip $-1/2 < \mathrm{Re}\,\zeta < 0$. To single out the *simple* pole $\zeta = 0$, we write

$$\int_{-1}^{1} \frac{\mathrm{d}s}{\sqrt{1-s^2}} f(s)[1+sA(s)]^{\zeta-1}(s^2)^{-\zeta-1/2} = 2f(0)$$

$$\times \int_{0}^{1} \frac{\mathrm{d}s}{\sqrt{1-s^2}} (s^2)^{-\zeta-1/2} + \mathcal{O}(1)$$

as $\zeta \to 0$, where $\mathcal{O}(1)$ is bounded. The last integral equals $\Gamma(-\zeta)\Gamma(1/2)/\,\Gamma(1/2-\zeta)$; thus,

$$\hat{I}_0(\zeta) \sim -2f(0)/\zeta \qquad \text{as } \zeta \to 0, \tag{C.3}$$

which yields the first term in each of (21) and (22). In the same vein, we find *zero* residue at $\zeta = 1/2$ and thus no contribution $\mathcal{O}(1/\delta)$ to $I_0(\delta^2)$.

Regarding the *double* pole of $\hat{I}_0(\zeta)$ at $\zeta = 1$, we write

$$f(s)[1+sA(s)]^{\zeta-1} = f(0) + s^2[\Lambda_0(s;\zeta) - \Lambda_0(0;\zeta)] + s^2\Lambda_0(0,\zeta) + \mathcal{K}_0(\zeta)s,$$

$$\Lambda_0(s;\zeta) = s^{-1}\left\{\frac{f(s)[1+sA(s)]^{\zeta-1} - f(0)}{s} - \mathcal{K}_0(\zeta)\right\},$$

$$\mathcal{K}_0(\zeta) = \lim_{s\to 0} \frac{f(s)[1+sA(s)]^{\zeta-1} - f(0)}{s}.$$

As $\tilde{\zeta} = 1-\zeta \to 0$, we have $\mathcal{K}_0(\zeta) \sim f'(0) - \tilde{\zeta} f(0)A(0)$ and

$$\Lambda_0(s;\zeta) \sim s^{-1}\left[\frac{f(s)-f(0)}{s} - f'(0)\right] - \tilde{\zeta}\frac{f(s)\ln[1+sA(s)] - sf(0)A(0)}{s^2};$$

hence, $\Lambda(0;\zeta) \sim \frac{1}{2}f''(0) - \tilde{\zeta}[f'(0)A(0) + f(0)A'(0) - \frac{1}{2}f(0)A(0)^2]$. By integration (in s), we obtain the Laurent expansion

$$\hat{I}_0(\zeta) \sim \frac{f+f''}{2\tilde{\zeta}^2} + \frac{1}{2\tilde{\zeta}}\left\{f + 2f'' - 2(fA)' + fA^2\right.$$

$$\left. - (f+f'')\left[\psi\left(\frac{3}{2}\right) + \psi\left(-\frac{1}{2}\right) - 2\psi(1)\right]\right\} \qquad \text{as} \quad \tilde{\zeta} \to 0, \tag{C.4}$$

where f, A and their derivatives are evaluated at $s = 0$. The residue for $\hat{I}_0(\zeta)(\delta^2)^{\zeta-1}$ at $\tilde{\zeta} = 0$ yields the remaining terms in expansions (21) and (22); $\ln(1/\delta^2)$ appears.

Integral I_1. The Mellin transform of $I_1(\delta^2)$ reads

$$\hat{I}_1(\zeta) = \frac{\Gamma(1-\zeta)\Gamma(\frac{1}{2}+\zeta)}{\Gamma(\frac{3}{2})} \int_{-1}^{1} \frac{\mathrm{d}s}{\sqrt{1-s^2}} sf(s)[1+sA(s)]^{\zeta-1}(s^2)^{-\zeta-1/2}$$

with the fundamental strip $-1/2 < \mathrm{Re}\,\zeta < 1/2$. Because of the factor s here, we conclude by analytic continuation that $\zeta = 1/2$ is a 'removable singularity'. Next, consider the *double* pole at $\zeta = 1$, setting $\tilde{\zeta} = 1-\zeta$. For analytic continuation, apply the splitting

$$f(s)[1+sA(s)]^{\zeta-1} = s[\Lambda_1(s;\zeta) - \Lambda_1(0;\zeta)] + s\Lambda_1(0;\zeta) + f(0),$$

where

$$\Lambda_1(s;\zeta) = \frac{f(s)[1+sA(s)]^{\zeta-1} - f(0)}{s}.$$

Note that $\Lambda_1(s;\zeta) \sim s^{-1}\{f(s) - f(0) - \tilde{\zeta} f(s)\ln[1 + sA(s)]\}$ as $\tilde{\zeta} \to 0$, uniformly in $s \in (-1, 1)$; in particular, $\lim_{s\to 0} \Lambda_1(s;\zeta) \sim f'(0) - \tilde{\zeta} f(0)A(0)$. By integration in s, we find

$$\hat{I}_1(\zeta) \sim \frac{f'(0)}{\tilde{\zeta}^2} + \frac{\mathcal{C}_1 + [2\psi(1) - \psi(\frac{1}{2}) - \psi(\frac{3}{2})]f'(0) + f(0)A(0)}{\tilde{\zeta}}, \tag{C.5}$$

as $\tilde{\zeta} \to 0$, where $\mathcal{C}_1 = \int_{-1}^{1} \mathrm{d}s\,(1 - s^2)^{-1/2}\{s^{-1}[f(s) - f(0)] - f'(0)\}|s|^{-1}$. The residue for $\hat{I}_1(\zeta)\,(\delta^2)^{\zeta-1}$ at $\tilde{\zeta} = 0$ yields expansions (23) and (24).

Integral I_2. The Mellin transform of $I_2(\delta^2)$ reads

$$\hat{I}_2(\zeta) = \frac{\Gamma(1-\zeta)\Gamma(\frac{1}{2}+\zeta)}{\Gamma(\frac{3}{2})} \int_{-1}^{1} \frac{\mathrm{d}s}{\sqrt{1-s^2}}[1 + sA(s)]^{\zeta-1} f(s)\,(s^2)^{-\zeta+1/2}, \tag{C.6}$$

with the fundamental strip $-1/2 < \mathrm{Re}\,\zeta < 1$. This function has a double pole at $\zeta = 1$. We analytically continue $\hat{I}_2(\zeta)$ to $1 \leqslant \mathrm{Re}\,\zeta < 3/2$ via the splitting

$$\Lambda_2(s;\zeta) := [1 + sA(s)]^{\zeta-1} f(s) = [\Lambda_2(s;\zeta) - \Lambda_2(0;\zeta)] + \Lambda_2(0;\zeta),$$

where $\Lambda_2(s;\zeta) \sim \{1 - \tilde{\zeta}\ln[1 + sA(s)]\}f(s)$ as $\tilde{\zeta} \to 0$. By substitution in (C.6), we find

$$\hat{I}_2(\zeta) \sim \frac{f(0)}{\tilde{\zeta}^2} + \frac{\mathcal{C}_2 + f(0)[2\psi(1) - \psi(\frac{1}{2}) - \psi(\frac{3}{2})]}{\tilde{\zeta}}, \tag{C.7}$$

where $\mathcal{C}_2 = \int_{-1}^{1} \mathrm{d}s\,(1 - s^2)^{-1/2}\,[f(s) - f(0)]|s|^{-1}$. The computation of the residue at $\tilde{\zeta} = 0$ for $I_2(\zeta)(\delta^2)^{\zeta-1}$ leads to expansions (25) and (26).

Integrals I_3, I_4. By contrast to $I_l(\delta^2)$ for $l = 0,\ 1,\ 2$, the integrals $I_3(\delta^2)$ and $I_4(\delta^2)$ remain convergent if $\delta = 0$ in the integrands. Thus, by continuity in δ, we have $I_3(\delta^2) \sim I_3(0)$ and $I_4(\delta^2) \sim I_4(0)$ as $\delta^2 \downarrow 0$, which readily yield (27) and (28).

References

[1] Jeong H-C and Williams E D 1999 *Surf. Sci. Rep.* **34** 171
[2] Marchenko V I and Parshin A Ya 1980 *Sov. Phys.—JETP* **52** 129
[3] Andreev A F and Kosevitch Yu A 1981 *Sov. Phys.—JETP* **54** 761
[4] Houchmandzadeh B and Misbah C 1995 *J. Phys. I (France)* **5** 685
[5] Tersoff J, Phang Y H, Zhang Z and Lagally M G 1995 *Phys. Rev. Lett.* **75** 2730
Xiang Y and E W 2004 *Phys. Rev.* B **69** 035409
Zhu X, Xu H and Xiang Y 2009 *Phys. Rev.* B **79** 125413
[6] Kukta R V, Peralta A and Kouris D 2002 *Phys. Rev. Lett.* **88** 186102
[7] Léonard F, Bartelt N C and Kellogg G L 2005 *Phys. Rev.* B **71** 045416
[8] Huang G-Y and Yu S-W 2007 *J. Appl. Mech.* **74** 821
[9] Burton W K, Cabrera N and Frank F C 1951 *Phil. Trans. R. Soc.* A **243** 299
[10] Weeks J D, Liu D-J and Jeong H-C 1997 *Dynamics of Crystal Surfaces and Interfaces* ed P M Duxbury and T J Pence (New York: Plenum) p 199
[11] Bonzel H P 2003 *Phys. Rep.* **385** 1
[12] Giesen M 2001 *Prog. Surf. Sci.* **68** 1
[13] Sasiela R J and Shelton J D 1993 *J. Math. Phys.* **34** 2572
[14] Cheng H and Wu T T 1987 *Expanding Protons: Scattering at High Energies* (Cambridge, MA: MIT Press)
[15] Pimpinelli A and Villain J 1998 *Physics of Crystal Growth* (Cambridge: Cambridge University Press)
[16] Tanaka S, Bartelt N C, Umbach C C, Tromp R M and Blakely J M 1997 *Phys. Rev. Lett.* **78** 3342
[17] Fok P-W 2006 *PhD thesis* MIT (Cambridge, MA: MIT Press)
[18] Israeli N and Kandel D 1998 *Phys. Rev. Lett.* **80** 3300
[19] Israeli N and Kandel D 1999 *Phys. Rev.* B **60** 5946
[20] Margetis D, Aziz M J and Stone H 2005 *Phys. Rev.* B **71** 165432

[21] Uwaha M and Watanabe K 2000 *J. Phys. Soc. Japan* **69** 497
[22] Margetis D and Kohn R V 2006 *Multisc. Model. Simul.* **5** 729
[23] Paulin S, Gillet F, Pierre-Louis O and Misbah C 2001 *Phys. Rev. Lett.* **86** 5538
[24] Krug J 2005 *Multiscale Modeling of Epitaxial Growth* ed A Voigt (Basel, Switzerland: Birkhäuser) p 69
[25] Eisenhart L P 1947 *An Introduction to Differential Geometry* (Princeton, NJ: Princeton University Press) pp 224–30
[26] Najafabadi R and Srolovitz D J 1994 *Surf. Sci.* **317** 221
[27] Eshelby J D 1956 *Solid State Phys.* **3** 79
[28] Prévot G and Croset B 2004 *Phys. Rev. Lett.* **92** 256104
Prévot G and Croset B 2006 *Phys. Rev.* B **74** 235410
[29] Jackson J D 1999 *Classical Electrodynamics* (New York: Wiley)
[30] Kubo R and Nagamiya T 1969 *Solid State Physics* ed R S Knox (New York: McGraw-Hill)
[31] Mott P H and Roland C M 2009 arXiv:0909.4697
[32] Bateman Manuscript Project 1953 *Higher Transcendental Functions* vol I, A Erdélyi (New York: McGraw-Hill)
[33] Bateman Manuscript Project 1953 *Higher Transcendental Functions* vol II, A Erdélyi (New York: McGraw-Hill)
[34] Carrier G F, Krook M and Pearson C E 1966 *Functions of a Complex Variable: Theory and Technique* (New York: McGraw-Hill)
[35] Bleistein N and Handelsman R A 1986 *Asymptotic Expansions of Integrals* (New York: Dover)
[36] Fikioris G 2006 *IEEE Trans. Antennas Propag.* **54** 3895